

Numerical modeling of magnetic field flow fractionation in microchannels : a two-fold approach using particle trajectories and concentration

J. Berthier*, P. Pham**, P. Massé*

* LETI (CEA-Technologies Avancées)- Département Systèmes-CSI
CEA Grenoble, 17 Avenue des Martyrs, 38054 Grenoble Cedex 9, France, jean.berthier@cea.fr

** Equipe Commune CEA-bioMérieux,
CEA Grenoble, 17 Avenue des Martyrs, 38054 Grenoble Cedex 9

1. ABSTRACT

Submicronic paramagnetic particles are currently used for biological applications like medical diagnostic [1]. Recently modeling of displacement of such particles has seen new developments like the calculation of the trajectory of a particle [2], or the calculation of the concentration of a great number of such particles, at the same time, in magnetic and hydrodynamic fields [3].

It is shown here that the two approaches – determinist and statistical - are consistent when applied to the calculation of a Magnetic Field-Flow Fractionation channel (MFFF) [4]: both numerical models predict similar convective patterns and the same accumulation location on the channel wall.

Moreover, the application to a MFFF shows that submicronic paramagnetic particles can be separated by such methods depending on their size and magnetic susceptibility.

2. INTRODUCTION

Field-flow fractionation (FFF) is a family of high resolution techniques for the separation of particles and polymers. Separation is achieved by the combined effects of a parabolic flow profile in the FFF channel and an external field which is applied perpendicularly to the channel .

Much work has been done in the domain of sedimentation field flow fractionation (SdFFF) [5]; however, recently, new applications for biological processes - like cell separation – have required the use of submicronic paramagnetic particles which are not much influenced by gravity but magnetic field-flow fractionation (MFFF or simply MF) is a well suited method to separate these particles according to their size and magnetic permeability [6],[7]. The principle of a MFFF is the same as that of a FFF, the force field being a vertical magnetic force field, as uniform as possible (fig 1).

Although models exist for the SdFFF channel [8], the approach is mainly experimental for MFFF.

Our first approach of the modeling of transport phenomena in MF is twofold : first, a determinist approach where trajectories of paramagnetic particles are determined ; second, a statistical approach in which concentration of paramagnetic particles is calculated. The focus of the present

modeling is the location of the center point of the particles build up at the capture wall.

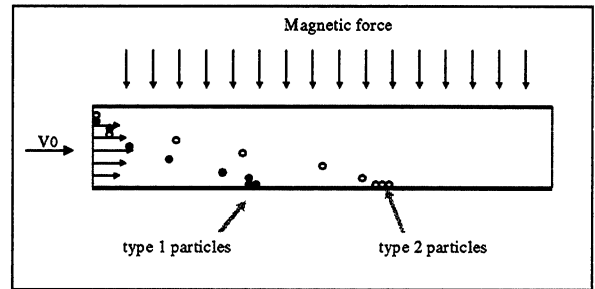


fig. 1. Schematic view of a MFFF. Particles trajectories depend on their radius and on their magnetic susceptibility (for a magnetic force field).

3. PARTICLE TRAJECTORY

Trajectories of paramagnetic particles are calculated by a force balance between magnetic, hydrodynamic and gravity forces

$$m \frac{d\vec{V}_p}{dt} = \vec{F}_{mag} + \vec{F}_{hyd} + \vec{F}_{grav} \quad (1)$$

where m is the mass of a particle and V_p its velocity.

In the present case, gravity and inertia are small compared to the magnetic and drag forces. The hydrodynamic drag is derived from the velocity field according to the equation

$$\vec{F}_{hyd} = -6\pi\eta r_h (\vec{V}_p - \vec{V}_f) \quad (2)$$

where η is the dynamic viscosity of the carrier fluid and r_h the hydrodynamic diameter of the particle. The velocity field is well known in the case of a laminar flow between two plates (the Reynolds number is much less than 1). The velocity profile across any section is parabolic and given by

$$\vec{V}_f = \frac{3V_0}{2} \left(1 - \frac{y^2}{d^2} \right) \hat{x} \quad (3)$$

where d is half the distance between the channel walls, \hat{x} is the unit vector of the horizontal axis and V_0 the average velocity. The magnetic force on a spherical particle ($r = r_h$) is given by

$$\vec{F}_{mag} = \frac{4}{3}\pi r \Delta\chi \sqrt{\left(\frac{1}{2}H^2\right)} \hat{y} \quad (4)$$

where $\Delta\chi$ is the difference of magnetic susceptibility between a particle and the fluid, H the magnitude of the magnetic field and \hat{y} the unit vector of the vertical downward oriented axis. Finally, the gravity term is simply

$$\vec{F}_{grav} = g v_p \Delta\rho \hat{y} \quad (5)$$

Substituting (2), (4) and (5) in (1) defines the trajectory.

We show here that, in the case where the particles are introduced in the flow section at the top near the upper plate (depletion wall), the trajectory can be calculated in a closed form. Simple algebra leads to the system

$$\begin{aligned} \frac{dV_{p,x}}{dt} &= -c_1 (V_{p,x} - V_{f,x}) \\ \frac{dV_{p,y}}{dt} &= -c_1 V_{p,y} + c_2 \end{aligned} \quad (6)$$

where the constants c_1 and c_2 are given by

$$\begin{aligned} c_1 &= \frac{6\pi\eta r}{m} \\ c_2 &= \frac{v_p \Delta\chi \sqrt{\left(\frac{1}{2}H^2\right)} + g v_p \Delta\rho}{m} \end{aligned}$$

Eq (6) admits a closed form solution for the velocity

$$\begin{aligned} V_{p,x} &= V_{p,x0} \exp(-c_1(t-t_0)) + V_{fx} [1 - \exp(-c_1(t-t_0))] \\ V_{p,y} &= V_{p,y0} \exp(-c_1(t-t_0)) + \frac{c_2}{c_1} [1 - \exp(-c_1(t-t_0))] \end{aligned} \quad (7)$$

where the subscript zero corresponds to the initial values. It can be shown that, if the velocity of the particle is zero at the inlet $V_{p,x} = V_{p,y} = 0$ (which is the case at the top, along the depletion wall), the time can be eliminated from (7) and the equation has the following solution

$$x = \frac{V_0}{2d^2} \frac{c_1}{c_2} [y(y^2 - 3d^2) - 2d^3] \quad (8)$$

with $x_0 = 0$, $y_0 = d$, $t_0 = 0$.

The distance where the particle touches the accumulation wall is given by

$$x_d = 2dV_0 \frac{c_1}{c_2} \quad (9)$$

where $\frac{c_1}{c_2}$ is the (non-dimensional) ratio of the hydrodynamic drag coefficient to the magnetic force coefficient. It can be readily checked that the larger the magnetic force, the smaller the distance x_d and the larger the hydrodynamic drag, the larger the distance x_d .

The separation distance between the accumulation sites on the accumulation plate for two different types of particles (1 and 2) is given by (10) - provided that the particles are sufficiently small to neglect the gravity force before the magnetic force

$$\frac{L_2}{L_1} = \frac{\Delta\chi_1}{\Delta\chi_2} \frac{r_1^2}{r_2^2} \quad (10)$$

where L is the distance from the channel entrance. Usually, smaller paramagnetic particles have lower magnetic susceptibility, so that there should be an efficient separation.

When the particles are introduced at any other location in the inlet, the solution for the trajectories requires numerical calculation based on a predictor-corrector method. A simple algorithm at the order 1 is sufficient because velocities are small. First, a prediction of the new coordinates of the particle at time t_{i+1} is given by

$$\begin{aligned} \tilde{x}_{i+1} &= x_i + \Delta t V_{pxi} \\ \tilde{y}_{i+1} &= y_i + \Delta t V_{pyi} \end{aligned} \quad (11)$$

then the velocity \tilde{V}_i at the predicted point is deduced from (7) and finally the following correction is made

$$\begin{aligned} x_{i+1} &= x_i + \Delta t \frac{\tilde{V}_{xi} + V_{xi}}{2} \\ y_{i+1} &= y_i + \Delta t \frac{\tilde{V}_{yi} + V_{yi}}{2} \end{aligned} \quad (12)$$

In the paragraph 5, trajectories calculated by either methods are shown.

4. PARTICLE CONCENTRATION

Concentration distribution is calculated by solving the mass conservation equation for the particles and the liquid, taking into account convection due to the flow and to the magnetic forces.

$$\frac{\partial c}{\partial t} = D\Delta c - \bar{v}\nabla c - u\bar{F}_{mag}\nabla c \quad (13)$$

where c is the concentration of particles, D the diffusion coefficient and u the mobility defined by

$$u = \frac{1}{6\pi\eta r} \quad (14)$$

Two types of numerical programs have been used to solve (13) : a 2-D Finite Difference program with a Crank-Nicholson scheme for diffusion terms and an upwind discretization for convective terms; and a 2-D Finite Element program using Nodal elements and Lagrange polynomials.

At the channel inlet, boundary conditions for the concentration are $c=c_0$ or $c=0$ depending on the location of particulate injection; and the condition $\frac{\partial c}{\partial n}=0$ at the channel outlet. The boundary conditions at the solid walls are

$$\begin{aligned} \bar{J}\cdot\bar{n} &= -D\text{grad}c\cdot\bar{n} + c\bar{v}\cdot\bar{n} + cu\bar{F}_{mag}\cdot\bar{n} \\ &= -D\text{grad}c\cdot\bar{n} + cu\bar{F}_{mag}\cdot\bar{n} = 0 \end{aligned} \quad (15)$$

5. NUMERICAL RESULTS

5.1. simulation of a MFFF

First, we examine the case of a MFFF channel of 100 μm width and 1 mm length. The fluid carrier is water and its average flow velocity is 0.1 mm/s. Particles are 1.4 μm of radius and 0.2 of magnetic susceptibility, their diffusivity is 1.53 $\mu\text{m}^2/\text{s}$ and the magnetic force is 3.45 pN .

Fig. 2 shows contour plots of the particles concentration compared to the calculated trajectories. The location of the injection is either at the top of the channel or at 1/3 of the vertical height. As expected, the isolines are centered on the trajectories: Brownian motion slightly displace the particles from their determinist trajectory.

The method has then been applied to the case of the separation of a colloid mixture containing two different types of submicronic paramagnetic particles (fig.3) differing by their magnetic susceptibility (0.2 and 0.8). Relation (10) applies even for trajectories not starting from the depletion wall.

Fig 4 shows the distribution of particles at the wall; the profile is nearly - but not quite - gaussian, owing to the fluid velocity. Dispersion of particles around the center location of the accumulation curve is larger for particles having travelled a longer path through the channel.

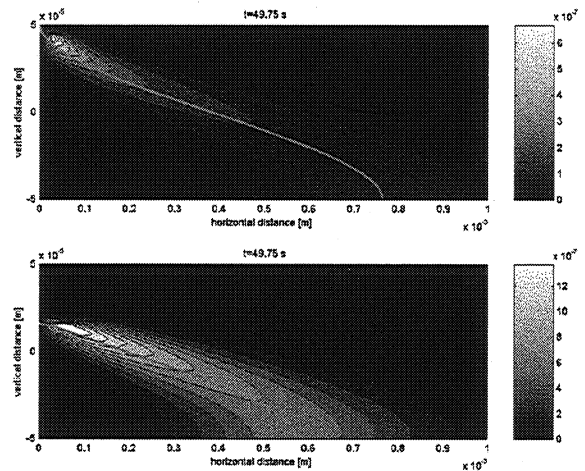


fig 2. Comparison of trajectories and concentration in a MFFF for two locations of injection. The trajectory of the first graph is calculated directly in a closed form (not to scale)

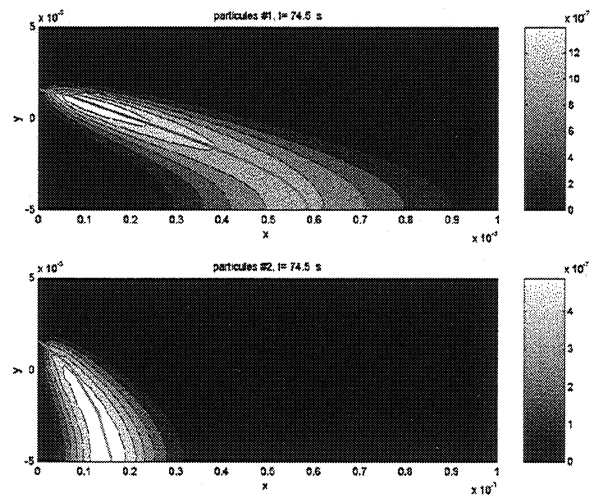


fig 3. Comparison between trajectories and concentration in a MFFF for two different types of paramagnetic particles (not to scale)

Carefull attention should be given to numerical false diffusion: the Finite Difference approach with upwind discretization has probably to much false diffusion whereas the Finite Element method used here seems to give more correct results. In the present case, it shows that nearly complete separation is achieved.

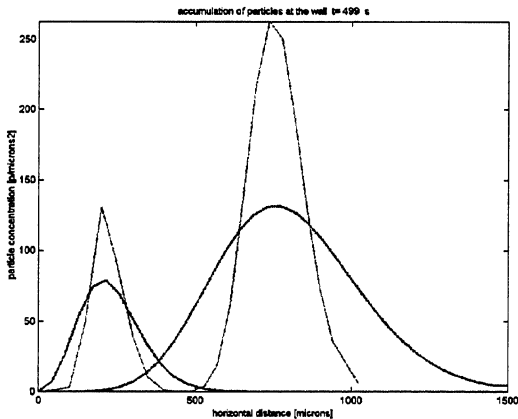


fig.4 : Wall concentration of particles of type 1 and 2 showing the separation of the two different samples. Thick line : Finite Differences calculation, thin line: Finite Elements calculation. Profiles are close but not quite gaussian. The longer the path through the channel, the greater the dispersion.

5.2. Simulation of a SPLITT channel

The SPLITT (split-flow thin cell fractionation) method is similar in its principle to the MFFF. The separation is being done this time at the flow outlet: depending on their size and magnetic susceptibility, the particles are confined at a certain vertical level in the channel. Higher velocities are used in the case of SPLITT. Fig 5 shows the calculated outlet flow rate of two types of paramagnetic particles (type 1: $\chi=0.2$ and $r=1.4\mu\text{m}$; type 2: $\chi=0.2$ and $r=0.14\mu\text{m}$).

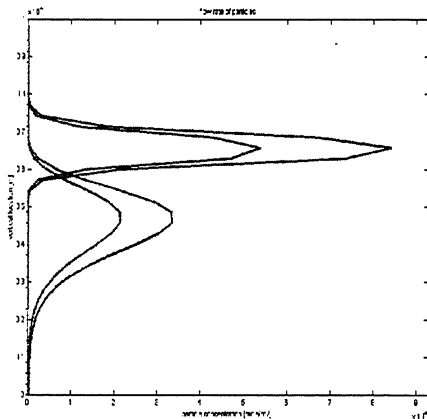


fig. 5: mass of particles of type 1 and 2 (at two different times) crossing the right boundary, showing the SPLITT separation of the two samples. Smaller particles show larger dispersion.

6. CONCLUSION

For the 2D case of a rectangular MFFF flow channel, it is shown here that the separation power of the fractionation for two types of particles (1 and 2) is proportional to $\frac{\Delta\chi_1 r_1^2}{\Delta\chi_2 r_2^2}$

where $\Delta\chi$ is the magnetic susceptibility difference between particles and carrier fluid and r the radius of a particle. Because usually the magnetic susceptibility of submicronic particles decreases with the radius, MFFF should ensure in most cases a satisfactory separation.

From a numerical point of view, the two approaches – trajectory and concentration – are consistent : isovalues of concentration are centered on the particles trajectories. However, concentration calculation shows that close attention should be paid to the effects of numerical false diffusion: too much false diffusion could lead to the erroneous conclusion that the separation is not complete.

In the oncoming work, focus will be on particles build up on the accumulation wall. Present results show that the profile of particles accumulation is close to gaussian, at least for small velocities.

7. REFERENCES

- [1] G. Giang, D. J. Harrison, " mRNA isolation for cDNA library construction on a chip," Micro Total Analysis Systems 2000, Kluwer Academic Publishers, pp 537-540, 2000.
- [2] P. Pham, P. Massé, J. Berthier, "Modélisation numérique de trajectoires de nanoparticules paramagnétiques sous l'action couplée multi-champs," NUMELEC 2000, 20-22 march 2000, Poitiers, France.
- [3] L.P. Davies, R. Gerber, "2D simulation of ultra-fine particle capture by a single-wire magnetic collector," IEEE Trans. On Magn., vol 26, n° 5, pp 1867-1869, 1990.
- [4] Y. Jiang, M.E. Miller, M.E. Hansen, M.N. Myers, P.S. Williams, "Fractionation and size analysis of magnetic particles using FFF and SPLITT technologies," Journal of Magnetism and Magnetic Materials, 194, pp 53-61, 1999.
- [5] R. Beckett, J. Ho, Y. Jiang, J.C. Giddings, "Measurement of mass and thickness of adsorbed films on colloidal particles by sedimentation field-flow fractionation," Langmuir, vol 7, n° 10, pp 2040-2047, 1991.
- [6] T. Rheinlaender, R. Koetitz, W. Weitschies, W. Semmler, "Different methods for the fractionation of magnetic fluids," Colloid Polym. Sci., 278, pp 259-263, 2000.
- [7] T. Rheinlaender, D. Roesner, W. Weitschies, W. Semmler, "Comparison of size-selective techniques for the fractionation of magnetic fluids," Journal of Magnetism and Magnetic Materials, 214, pp 269-279, 2000.
- [8] M.E. Hansen, J.C. Giddings, R. Beckett, " Colloid characterization by sedimentation field-flow fractionation," J. of Colloid and Interface Science, vol 132, n° 2, pp 300-312, 1988.